THE EFFECT AND CONTRIBUTION OF WIND GENERATED ROTATION ON OUTLET TEMPERATURE AND HEAT GAIN OF LS-2 PARABOLIC TROUGH SOLAR COLLECTOR

by

*Omid Karimi Sadaghiyani[*1], Seyed Mehdi Pesteei[1], Iraj Mirzaee[1]*

[1]Department of Mechanical Engineering, Urmia University, Urmia, Iran
E-mail: o.sadaghiyani@urmia.ac.ir
E-mail:spesteei@yahoo.com
Email: i.mirzaee@urmia.ac.ir

The Monte Carlo ray tracing method is applied and coupled with finite volume numerical methods to study effect of rotation on outlet temperature and heat gain of LS-2 parabolic trough concentrator (PTC). Based on effect of sunshape, curve of mirror and use of MCRT, heat flux distribution around of inner wall of evacuated tube is calculated. After calculation of heat flux, the geometry of LS-2 Luz collector is created and finite volume method is applied to simulate. The obtained results are compared with Dudley et al test results for irrotational cases to validate these numerical solving models. Consider that, for rotational models ,the solving method separately with K.S. Ball's results. In this work, according to the structure of mentioned collector, we use plug as a flow restriction. In the rotational case studies, the inner wall rotates with different angular speeds. We compare results of rotational collector with irrotational. Also for these two main states, the location of plug changed then outlet temperature and heat gain of collector are studied. The results show that rotation have positive role on heat transfer processing and the rotational plug in bottom half of tube have better effectual than upper half of tube. Also the contribution of rotation is calculated in the all of case studies. Working fluid of these study is one of the oil derivatives namely Syltherm-800. The power of wind can be used to rotate tube of collector.
Key words: *Parabolic trough collector, LS-2 collector, Contribution of rotation, Outlet temperature.*

1. Introduction

Since the 1970s, many simulations and experiments on solar systems were published, especially on the parabolic trough concentrator (PTC). The purpose of some of them was reduction on costs and increasing of performance by new designs, others had been applied to improving the reliability of receiver tubes, and selective coating performance [19,20]. After these developments of experiments on solar systems, the numerical studies were performed widely [4]. Most of these studies

are one dimensional and based on the first law of thermodynamics [3,8] or based on second law [18,21]. Two dimensional efficiency analysis models were developed recently [6,8].

As early as in 1977, analytical modeling of parabolic trough concentrator was used by Evans [14] and Harris et al[15]. Then, Sheldon M.jeter [1,2] calculated a first integral of the concentrated radiant heat flux density for linear parabolic collectors. Sundia National Research Laboratory (SNRL) specified the thermal loss and collector efficiency of the LS-2 SEGS trough collector (1994) [3]. An optical model of the parabolic trough concentrator has been improved by Heinzel et al (1995) [4].

The solar rays after reflecting from parabolic surface focus on outer wall of absorber tube. In this work, heat flux distribution around of tube is calculated by the in-house developed code based on the Monte Carlo Ray Tracing method [9]. Consider that the sun rays were assumed nonparallel. Three dimensional finite volume numerical modeling applied and coupled with MCRT method to simulate LS-2 solar collector that tested at Sandia National Research Laboratory. In this work, we try to study effect of rotation on heat transfer characteristics such as outlet temperature and heat gain compared with irrotational walls. In these case studies the inner wall (plug) of collector rotated respectively. The power source of rotation is wind force.

2. Model description

To be able to validate the MCRT method for signification of flux distribution that is function of structural and geometrical parameters, results are compared with Jeter's analytical results. Also in order to validate of finite volume numerical methods, results are compared with Dudley et al results [3] and K.S. Ball [22]. According to following table, the structural properties of mentioned collector are:

Table(1):the list of LS-2collector structural properties.

LS-2 PTC(as tested as SNRL):	
Manufacturer:	Luz industrial-israel
Operating temperature:	100-400°C
Module size:	7.8 m $\times$ 5 m
Rim angle:	70 degrees
Reflector:	12 thermally sagged glass panel
Aperture area:	39.2 m^2
Focal length:	1.84 m
Concentration ratio:	22.74
Receiver:	Evacuated tube, metal bellows at each end
Absorber diameter:	70 mm
Glass cover:	
Diameter:	115 mm
Transmittance:	0.95
Absorber surface:	Cermet selective surface
Absorptance:	0.96
Absorber tube inner diameter:	66 mm
Absorber tube outer diameter:	70 m

3. Governing equations

As the test conditions, the fluid flow is turbulence and in steady state condition. So the governing equations for continuity, momentum, standard k-ε and energy are fundamental equations for turbulence models can be written as follows:

Continuity:

$$\frac{\partial}{\partial x_i}(\rho u_i) = 0 \tag{1}$$

Momentum equation:

$$\frac{\partial}{\partial x_i}(\rho u_i u_j) = -\frac{\partial p}{\partial x_i} + \frac{\partial}{\partial x_i}\left[(\mu_t + \mu)\left(\frac{\partial u_i}{\partial x_j} + \frac{\partial u_j}{\partial x_i}\right) - \frac{2}{3}(\mu_t + \mu)\frac{\partial u_i}{\partial x_i}\delta_{ij}\right] + \rho g_i \tag{2}$$

Energy equation:

$$\frac{\partial}{\partial x_i}(\rho u_i T) = \frac{\partial}{\partial x_i}\left[\left(\frac{\mu}{Pr} + \frac{\mu_t}{\sigma_T}\right)\frac{\partial T}{\partial x_i}\right] + S_R \tag{3}$$

k equation:

$$\frac{\partial}{\partial x_i}(\rho u_i k) = \frac{\partial}{\partial x_i}\left[\left(\mu + \frac{\mu_t}{\sigma_k}\right)\frac{\partial k}{\partial x_i}\right] + G_k - \rho\varepsilon \tag{4}$$

ε equation:

$$\frac{\partial}{\partial x_i}(\rho u_i \varepsilon) = \frac{\partial}{\partial x_i}\left[\left(\mu + \frac{\mu_t}{\sigma_\varepsilon}\right)\frac{\partial \varepsilon}{\partial x_i}\right] + \frac{\varepsilon}{k}(c_1 G_k - c_2\rho\varepsilon) \tag{5}$$

where the turbulence viscosity and the production rate expressed by:

$$\mu_t = C_\mu \rho \frac{k^2}{\varepsilon} \tag{6}$$

$$G_k = \mu_t \frac{\partial u_i}{\partial x_j}\left(\frac{\partial u_i}{\partial x_j} + \frac{\partial u_j}{\partial x_i}\right)$$

The standard constants are used c_μ =0.09, c_1 = 1.44, c_2 =1.92, σ_k=1.0, σ_ε=1.3, and σ_T=0.85.

4. Boundary conditions

The boundary conditions that are applied to the inlet and outlet of collector tube:
For inlet:

$\dot{m}_x$=0.6782 kg/sec $\dot{m}_y$=$\dot{m}_z$=0 kg/sec T_{in}=375.5°K

$\mu_t = 1\% . 1/2 u_{in}^2, \varepsilon_{in} = c_\mu . \rho(T) . k_{in}^2/\mu_t$, where $c_\mu = 0.09$, $\mu_t = 100$ [23]

Also mass flow inlet boundary condition has been applied.

For outlet:

fully-developed assumption and outflow boundary conditions.

The amount of direct normal incident that used to simulated sun rays is 933[Wm^2]. The heat transfer fluid (HTF) is Syltherm-800 liquid oil that its properties are functions of temperature:
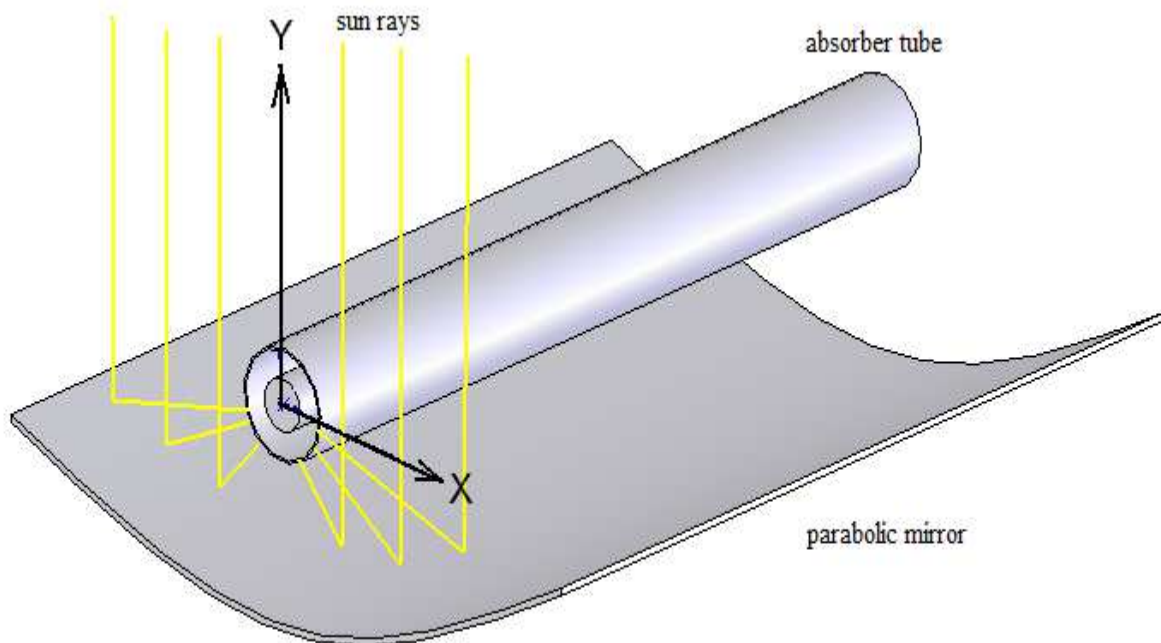
$$c_p = 0.00178T + 1.107798 \ [\text{kj kg}^{-1}\text{K}^{-1}] \tag{7}$$

$$\rho = -0.4153495T + 1105.702 \ [\text{kg}m^{-3}] \tag{8}$$

$$k = -5.753496 \times 10^{-10}T^2 - 1.875266 \times 10^{-4}T + 0.1900210 \ [\text{W}m^{-1}K^{-1}] \tag{9}$$

$$\mu = 6.672 \times 10^{-7}T^4 - 1.566 \times 10^{-3}T^3 + 1.388T^2 - 0.05541T + 8.487 \times 10^4 [\mu Pa.sec] \tag{10}$$

The substance of solid material is stainless steel-304 with conductivity 54 [W$m^{-1}K^{-1}$].

Fig(1) shows the parabolic trough collector and sun rays schematically.

Thermal boundary condition around of tube is function of θ in polar coordination system that two conditions is calculated. The sun rays are converged or assumed parallel. In this article, the heat flux of converged rays is applied and used to simulated LS-2 collector. Consider that the angle of convergence is 16°.
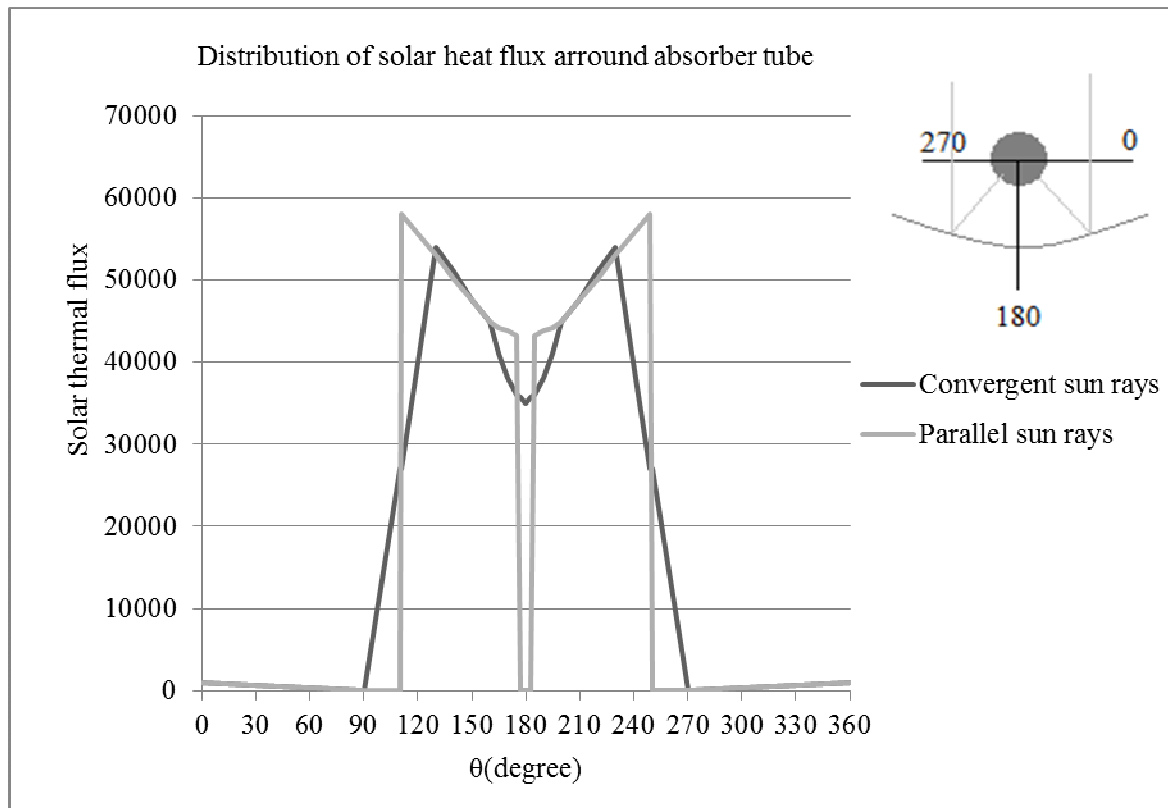
Fig(2): Schematics of heat flux distribution around receiver tube

5. Numerical methods

Several mesh systems are generated to test independent of grids. These grid systems contain $(N_C=70, N_Z=340), (N_C=70, N_Z=4300), (N_C=70, N_Z=500)$ and $(N_C=90, N_Z=340)$. Obtained results showed good agreement together.

The fundamental equations were discretized by the finite volume method[22main] and the convective terms in momentum and energy equations were discretized with the second upwind scheme. The SIMPLE algorithm was applied to coupling between velocity and pressure. Consider that the convergence criterion for the velocity and energy was the maximum residual of the first 10 iterations was less than 10^{-5} and 10^{-7} respectively. The results of numerical simulation compare with Dudley et al experimental results,

Table(2):Conditions of environment and comparing of numerical and experimental results together.

Table(1): The list of LS-2 parabolic system.

Case study	DNI (w/m^2)	MASS FLOW RATE(L/min)	AIR TEMP (°C)	INLET TEMP(°C)	OUTLET TEMP(°C) EXP	OUTLET TEMP(°C) NUM	η Efficiency NUM%
1	933.7	47.7	21.2	102.2	124.0	124.2	72.07
2	982.3	49.1	24.3	197.5	219.5	220.4	71
3	909.5	54.7	26.2	250.7	269.4	271	70.5
4	937.9	55.5	28.8	297.8	316.9	318	68.5

so the solving method is validated and used for others studies that we change angular speeds of outer wall or plug rotation with several position of plug**.** The working fluid of these studies is Syltherm-8oo and the kind of tube and plug is stainless steel 304. The applied angular speeds that have been used in work, are 10,20 and 50 rad/sec. For preparation of these speeds we can use from little wind tools. If we use overdriver gear boxes that change low angular speeds to high and uniform angular speeds then, the power of wind is used on heat transfer processing. The X axis in diagrams are non-dimensional displacement of plug from tube center that is defined as:

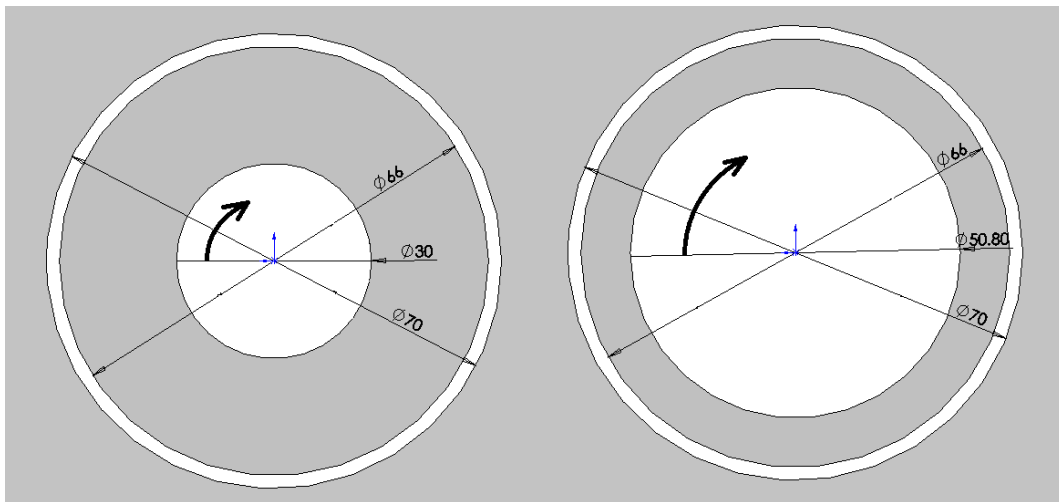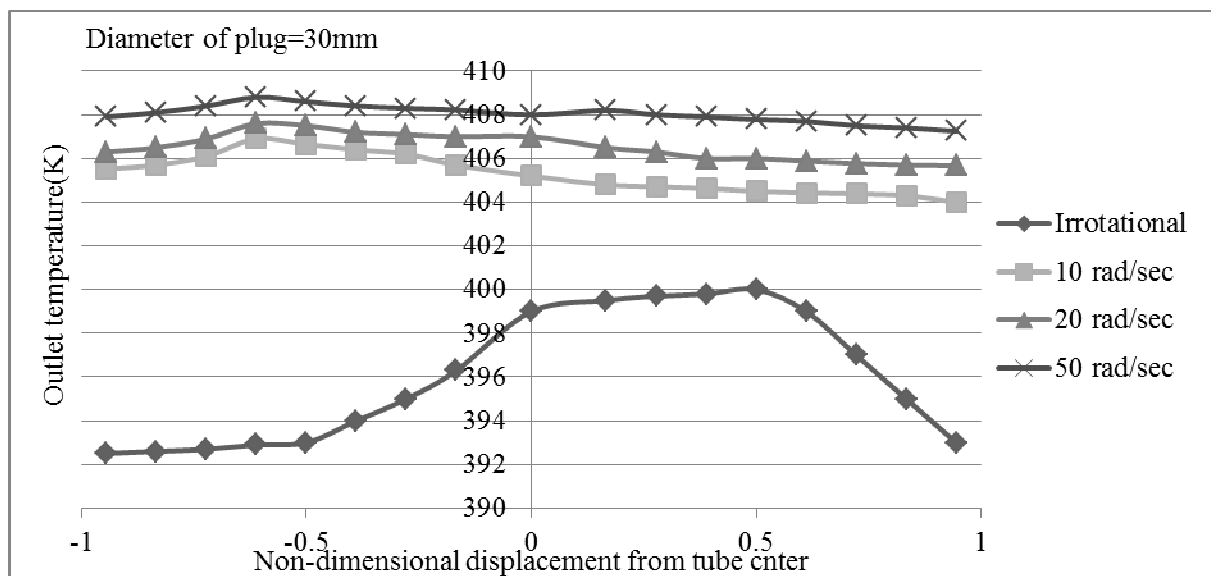$$\text{Non-dimensional displacement} = 2d_p/(D_i - D_p)$$

Fig (3):Cross sections of absorber tubes and their plugs(30 and 50.8mm respectively) .

Results of these case studies are given as follows:

Fig(4) shows a diagram of outlet temperature for D_p=30mm with angular speeds=10,20 and 50 rad/sec comparing with irrotational case:

Fig(4):Effect of rotation and position of plug on outlet temperature(diameter of plug=30mm)

Obviously, at irrotational case, it is found that, for non-dimensional displacement=0.5, maximum outlet temperature can be reached, but at rotational cases, this maximum temperature locate at non-dimensional displacement = -0.5 . Other conclusion that we obtain, it is that for high angular speeds, the displacement of plug have low effect rather than low angular speeds. These results are so similar to other diameters results, such as 50.8. In this figure, regard all of diagrams sperately specially the variation between maximum and minimum outlet temperature points. It is cancluded that, on high angular speeds, the impressibility of outlet temperature from location is low and if the angular speed increases likewise, the trand of diagram will be constant function. The variation between each of rotational cases with irrotational, show the effect of rotation on heat transfer processing. These influences are shawn in diagram of plug that its diameter is 50.8mm.

Fig(5) shows a diagram of outlet temperature for D_p=50.8mm with angular speeds=10,20 and 50 rad/sec comparing with irrotational case:
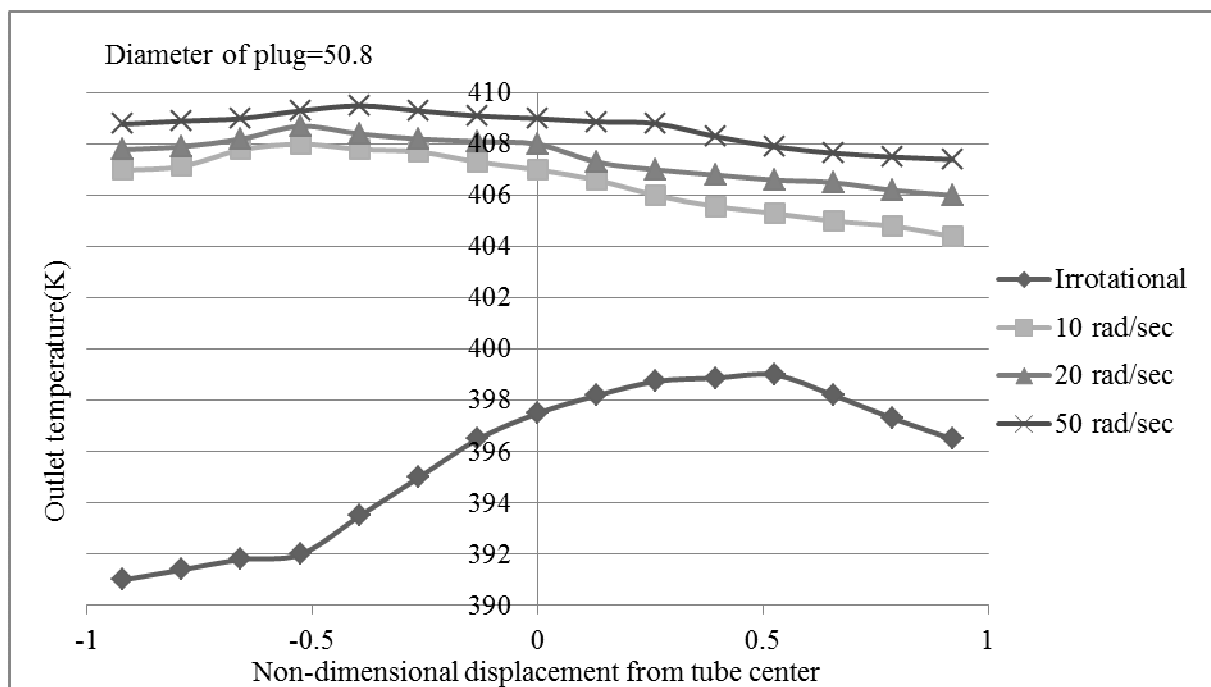
Fig(5):Effect of rotation and position of plug on outlet temperature(diameter of plug=50.8mm)

In the other study, effect of diameter on heat transfer is analyzed, so if diameter of plug increases, collecting of solar energy will be improved. Fig (6) shows the effect of diameter of plug on outlet temperature. In this figure, at the left of irrotational case, the trend of diagram is decreasing, because, in the low diameters, the natural convection is very effective role on good mixing of flow. But on the rotational plugs effects of natural convection is negligible. Considering this convergence of diagrams at right hand, it is understood, increasing the angular speed at low diameters is more effective than high diameters.
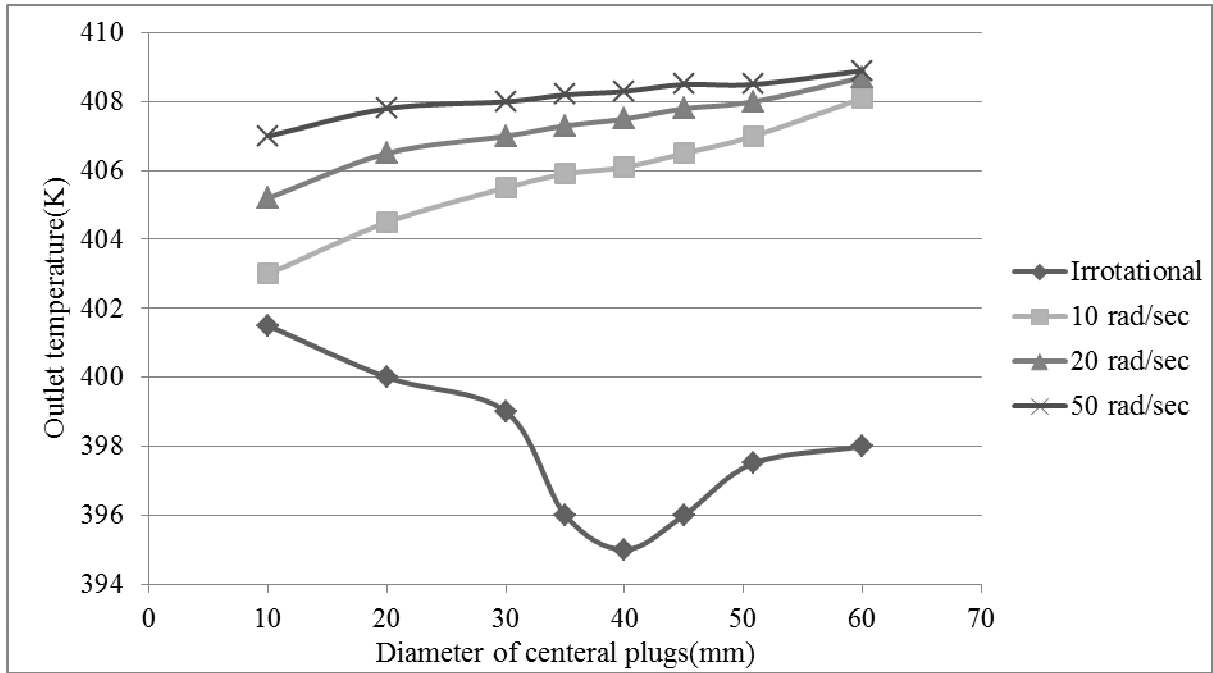
Fig(6): Effect of diameter on outlet temperature for central plugs

6. Thermal efficiency and amount of heat gain

The useful heat gain by the parabolic trough collector exposed to solar radiation with measured values of inlet and outlet temperatures and mass flow rate ($\dot{m}$) and specific heat of fluid (c_p) is defined as:

$$Q_u = \dot{m} c_p (T_o - T_i) \tag{11}$$

Where the efficiency of t0he collector is calculated by:

$$\eta_{th} = {Q_u}/{A_c . I} \tag{12}$$

Where A_c is the area of the collector and I is the solar radiation incident on the collector mirror. If the power of wind act on the solar systems via mill then the relation of efficiency is changed as:

$$\eta_{th} = {Q_u}/{(A_c . I + wind\ energy)} \tag{13}$$

This formula needs the calculated amount of wind energy. But for good comparison with irrotational case, we present a relation as:

$$Percent\ of\ heat\ gain\ toward\ approached\ solar\ heat = {Q_u}/{A_c . I} \tag{14}$$

The effect of rotation and its angular speeds and location on the heat gain were calculated, the following diagrams show amounts of outflow temperature and heat gain toward approached solar heat, after applying these changes for D_u =30mm and 50.8mm respectively:
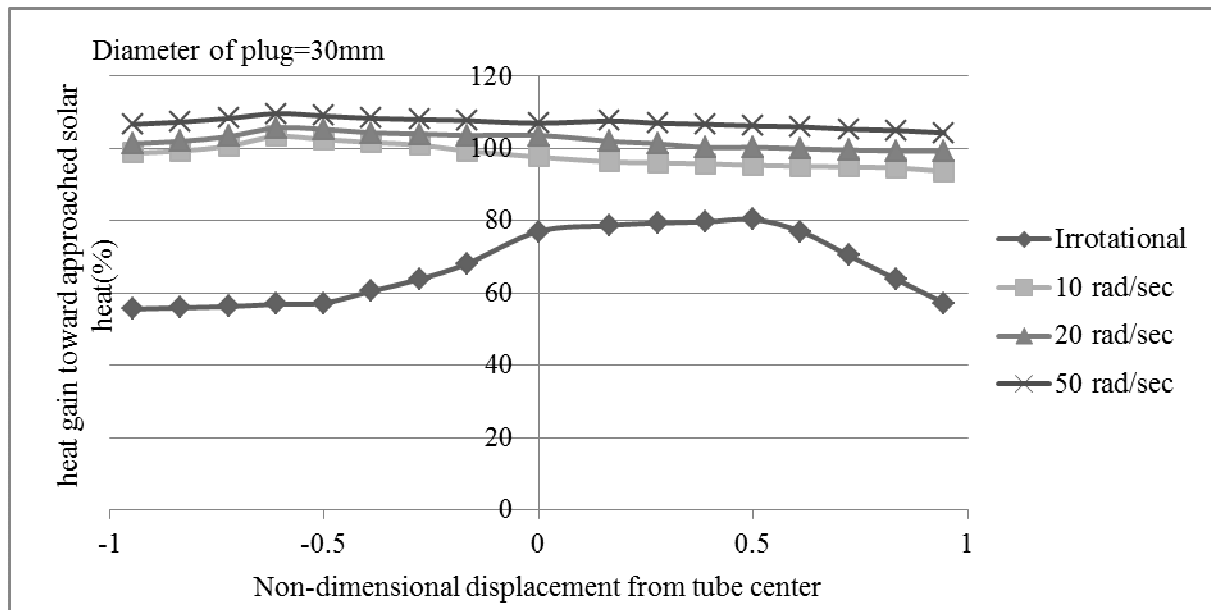

Fig (7):Comparison between rotational inner wall with various angular speeds and irrotational walls.

Obviously, the variation between maximum and minimum points for each of diagrams show that on high angular speeds, the impressibility of energy collecting and heat gain from plug location is low and if the angular speed likwise increase the trand of diagram will be constant function. As the maximum variation happen in irrotational case study. The variations between each of rotational cases diagrams with irrotational diagram, show the effect of rotation on heat transfer processing. These influences are shawn in diagram of fig(8) that its diameter is 50.8mm.
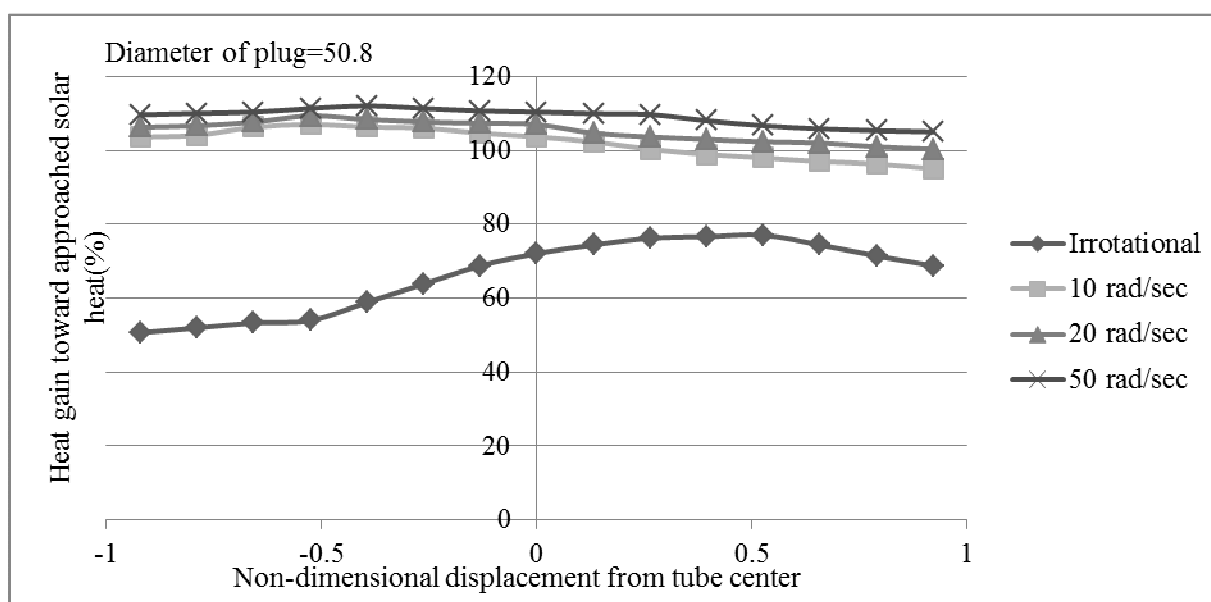
Fig(8):Diagram of heat gain toward approached solar heat

We use from rotated central plugs with several diameters, it is concluded that, if the diameter of plug increase, effect of angular speed will be pale, unlike irrotational case.
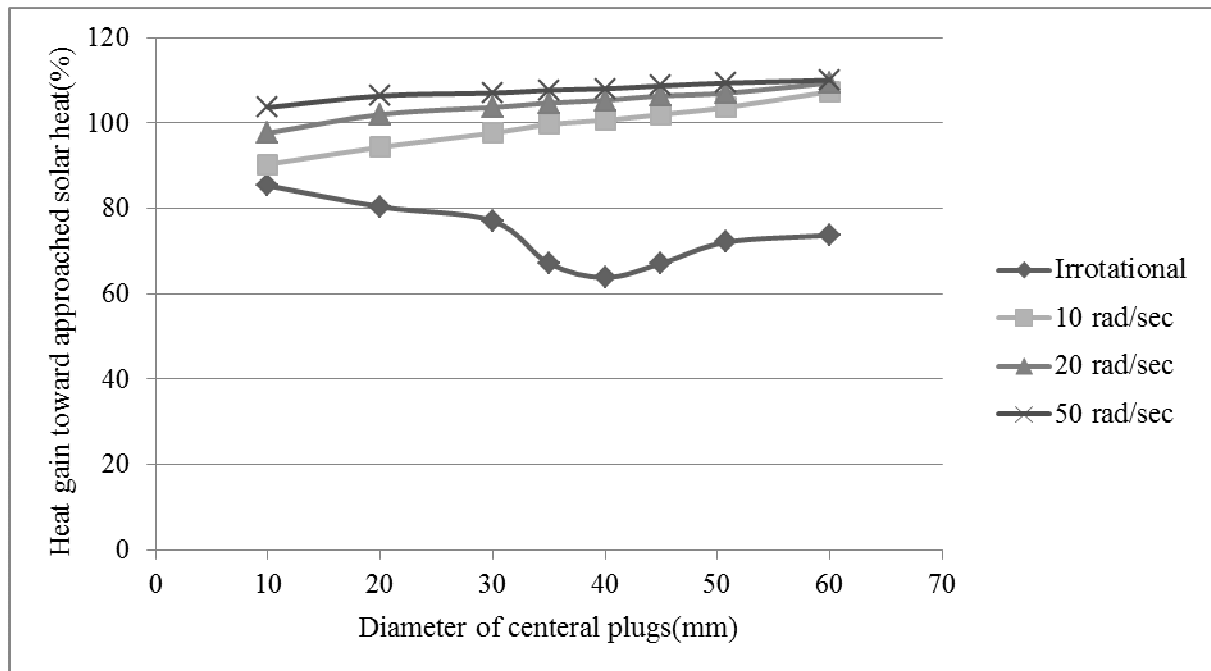
Fig(9):Diagram of heat gain toward approached solar heat for central plugs.

7. Contribution of rotation on heat transfer processing

We present one relation that expresses contribution of rotation on heat transfer processing, because both of the solar energy and the wind energy contribute on heat transfer processing. Solar energy via heat flux generation and wind energy via rotation. The rotation has two effects on process: firstly, mixing and so increasing of Nusselt-number, secondly, heat generation due to friction. So we try to know effect of rotation and its contribution on heating of liquid oil.
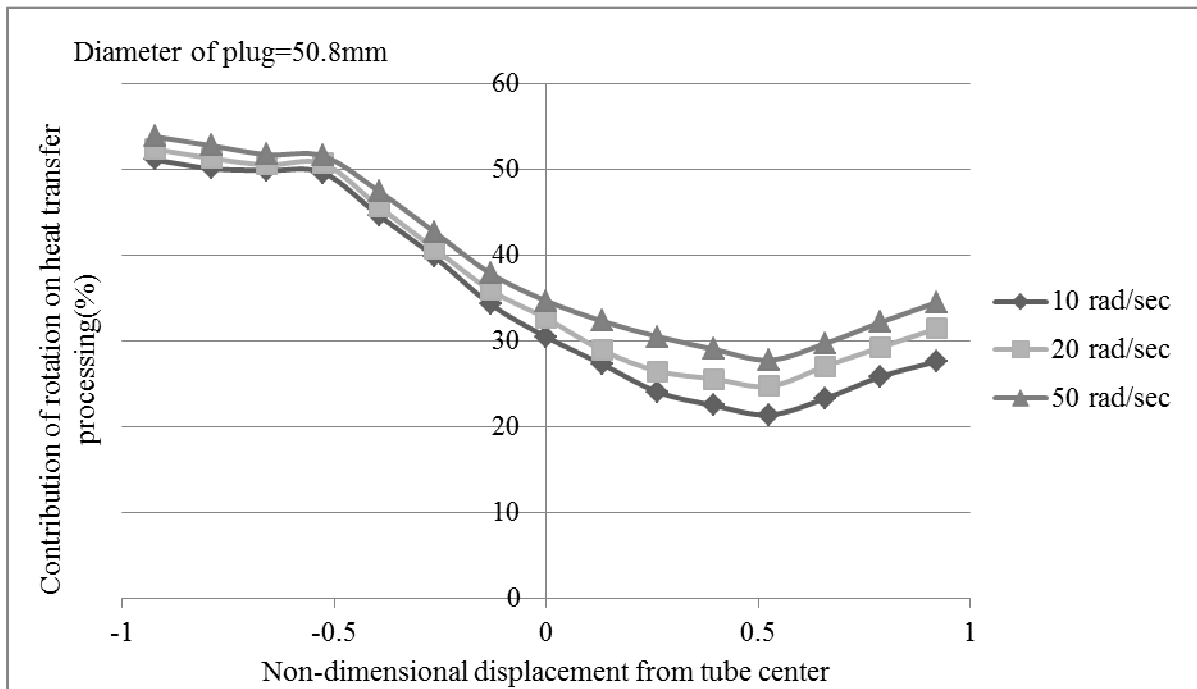
Contribution of rotation on heat transfer processing=$\frac{(Q_{rot} - Q_{irr})}{Q_{rot}}$ (15)

Consider that the each of Q_{rot} and Q_{irr} are calculated via $Q = \dot{m}c_v(T_o - T_i)$. (16)

After calculation the contribution of rotation on heat gain can be reached. These results are shown in figs (10),(11) and(12).
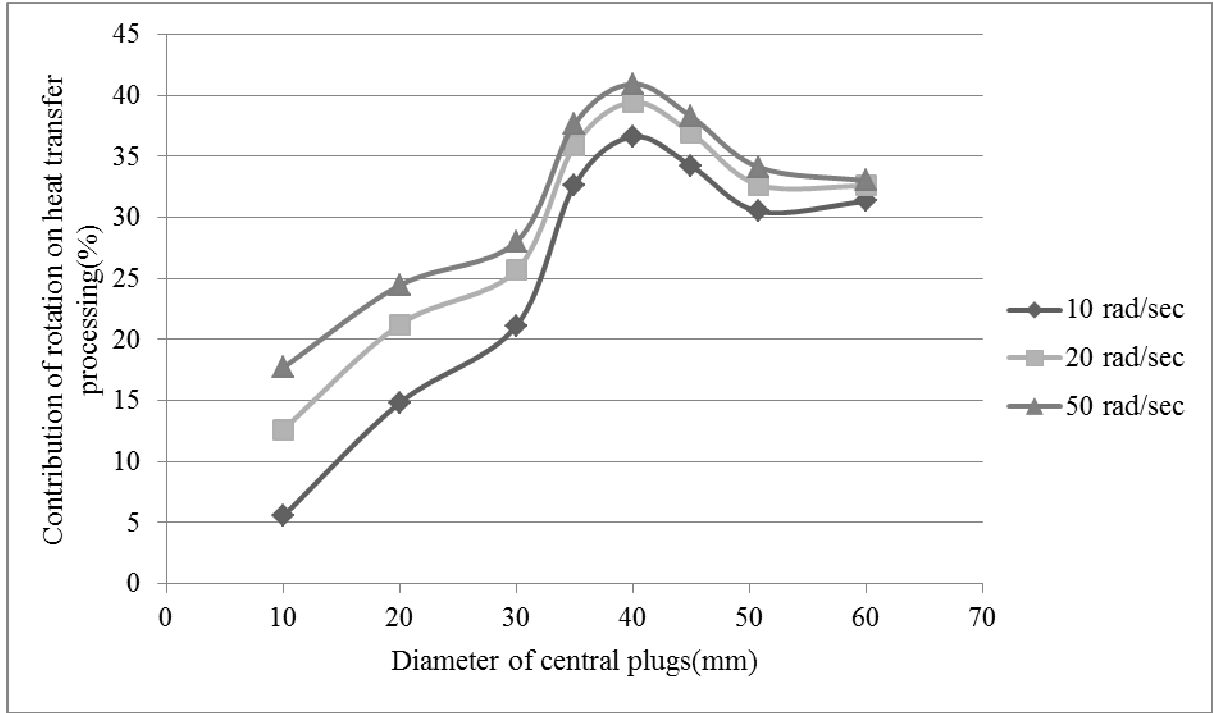
10
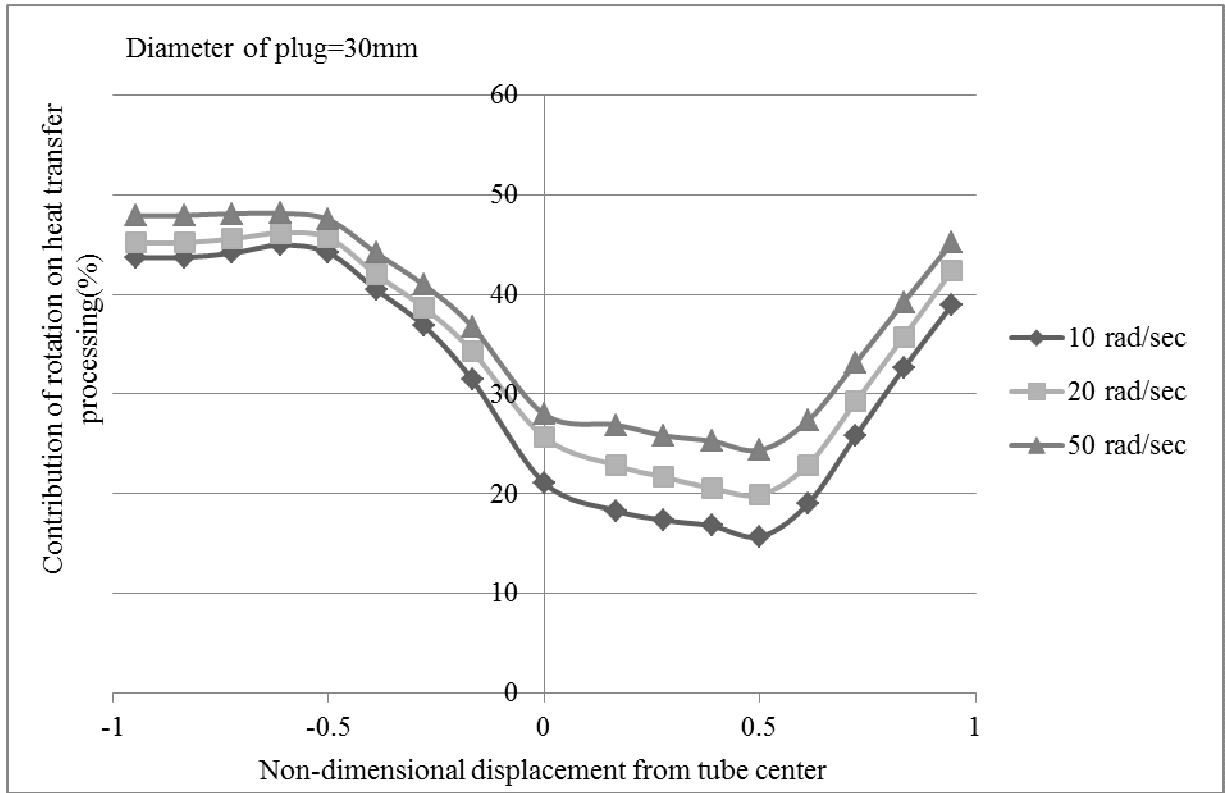
Fig(10):Contribution of rotation on heat transfer processing for plug with diameter=30mm

Fig(11): The contribution of rotation on heat transfer processing for plug with diameter=50.8mm

Also the contribution of rotation on heat transfer processing for the central plugs with several diameters are calculated in fig (12) these effects are shown clearly:

Fig(12):Contribution of rotation on heat transfer processing for central plugs

8. Conclusion

In this work, three-dimensional analysis of heat transfer characteristics in the evacuated tube is performed by coupling the MCRT and numerical simulation methods. Three parameters selected to change (diameter of plug, location of plug and angular speeds). The aims of these changes are study of outlet temperature and efficiency of collectors. Notice that likely when the amount of non-dimensional displacement of irrotational plug from tube center=0.5, then the maximum outlet temperature and efficiency can be reached. Also, for rotational states, the maximum outlet temperature and efficiency located at non-dimensional displacement = -0.5 . It is the other conclusion that increasing the angular speed at low diameters is more effective than high diameters. In this work, we studied effect of wind energy in outlet temperature and analyzed contribution of rotation on heat transfer processing at parabolic trough collectors. This study says that if the wind contributes in heat transfer, outlet temperature will be increase 10% until 60%. Also at D_p =40mm, the contribution of rotation in heat transfer is most.

9. Nomenclature

A_c aperture area

c_μ, c_1, c_2 coefficients in the turbulence model

I_b direct normal irradiance [Wm^{-2}]

K   incident angle modifier

Pr   Prandtl number

q_{loss} thermal loss [Wm^{-2}]

12

q_{mass} flow rate [kgs^{-1}]

Q_u usefull heat gain

Q_{rot} heat gain in rotational state

Q_{irr} heat gain in irrotational state

Re   Reynolds number based on tube hydraulic diameter

S_R additional source term [Wm^{-3}]

T   temperature (K)

ΔT_{ab} receiver fluid temperature above ambient air temperature [K]

u, v,w x, y, z   velocity components [ms^{-1}]

x, y, z   Cartesian coordinates

Greek symbols

μ   dynamic viscosity [Pa s]

μ_t turbulent viscosity [Pa s]

κ   thermal conductivity or kinetic energy

ε   turbulent dissipation rate or emissivity

σ_T turbulent Prandtl number

$\sigma_k, \sigma_\varepsilon$ turbulent Prandtl numbers for diffusion of k and ε

ν   kinematic viscosity [$m^2 s^{-1}$]

ρ   density [kg m^{-3}]

η   collector efficiency calculated by test data

η′   collector efficiency calculated by simulation data Subscripts

a   ambient

in   inlet parameters

m   mean or average value

o   outlet parameters

10. References

[1]   S.M. Jeter, "Calculation of the concentrated flux distribution in parabolic trough collectors by a semifinite formulation", *Solar Energy*,.37 (1986), pp.335-345.

[2]   S.M. Jeter, "Analytical determination of the optical performance of parabolic trough collectors from design data", *Solar Energy*,.39 (1987), pp.11-21

[3]   V. Dudley, G. Kolb, M. Sloan, D. Kearney, SEGS LS2 solar collector — test results, Report of Sandia National Laboratories, SANDIA94-1884, USA, (1994).

[4]   V. Heinzel, H. Kungle, M. Simon, Simulation of a Parabolic Trough Collector, *ISESSolar World Congress, Harare, Zimbabwe*, (1995) pp. 1–10.

[5]   N. Naeeni, M. Yaghoubi, Analysis of wind flow around a parabolic collector (1) fluid flow, *Renewable Energy* 32 (2007) pp.1898–1916.

[6]   N. Naeeni, M. Yaghoubi, Analysis of wind flow around a parabolic collector (2) heat transfer from receiver tube, *Renewable Energy* 32 (2007) pp. 1259–1272.

[7]   Dudley VE,Workhoven RM. Performance testing of the Solar Kinetics T-700A Solar Collector. Tech. Rep. No.SAND81-0984. Albuquerque: SANDIA; (1982).

[8]   R. Forristall, Heat Transfer Analysis and Modeling of a Parabolic Trough Solar Receiver Implemented in Engineering Equation Solver, Technical Report, NREL/ TP-550-34169, October, (2003).

[9]   J. Xiao, Y.L. He, Y.B. Tao, R.J. Xu, Simulation for Concentrating Characteristics of Parabolic Solar Collector Part A: Analysis of Concentrating Characteristics, *14th Annual Symposium of Chinese Society of Engineering Thermophysics*, Tianjin, China, (2008).

[10] S.D. Odeh, G.L. Morrison, M. Behnia, Thermal analysis of parabolic trough solar collector for power generation, In Proceedings of ANZSES *34th Annual Conference*, Darwin, Australia, (1996) pp. 460–467.

[11] Y. Shuai, X.L. Xia, H.P. Tan, Radiation performance of dish solar concentrator/ cavity receiver systems, *Solar Energy* 82 (1) (2008) pp.13–21.

[12] Romero M, Martı´nez D, Zarza E. Terrestrial solar thermal power plants: on the verge of commercialization. In: 4th intconf on sol power from space; (2004).

[13] Pytlinski JT. Solar energy installations for pumping irrigation water. *Solar Energy* (1978) [Review paper].

[14] Evens DL. On the performance of cylindrical parabolic solar concentrators with flat absorbers. *Solar Energy 19* (1977).

[15] Harris James A, Duff William S. Focal plane flux distribution produced by solar concentrating reflectors. *Solar Energy* 27 (1981).

[16] Pytlinski JT. Solar energy installations for pumping irrigation water. *Solar Energy* 21 (1978) [Review paper].

[17] Kreider JF, Kreith F. Solar energy handbook. New York: McGraw Hill; (1981).

[18] N. Eskin, Transient performance analysis of cylindrical parabolic*, Energy Convers*. Manage. 40 (1999) pp. 175–191.

[19] H. Price, E. Lüpfert, D. Kearney, E.Zarza, rt al., Advances in parabolic trough solar power technology,J. *solar energy* (2002) pp. 109-125**.**

[20] S.A. Kalogirou, Solar thermal collectors and applications, Prog. Energy Combust. Sci. 30 (2004) pp. 231-295.

[21] S.K. Tyagi, S.W. Wang, M.K. Singhal, S.C. Kaushik, S.R. Park, Exergy analysis and parametric study of concentrating type solar collectors, *International journal of Thermal Science* 46 (2007) pp. 1304-1310**.**

[22] K.S. Ball, B. Farouk, V.C. Dixit**,** An experimental study of heat transfer in a vertical annulus with a rotating inner cylinder**,** (1989) *International Journal of Heat and Mass Transfer* 32 (1989) pp. 1517-1527**.**

[23] W.Q. Tao, Numerical Heat Transfer, second ed, Xi'an Jiaotong University Press, Xi'an (2001)**.**